

# Selective DNA and Protein Isolation from Marine Macrophyte Surfaces

Marino Korlević<sup>1\*</sup>, Marsej Markovski<sup>1</sup>, Zihao Zhao<sup>2</sup>, Gerhard J. Herndl<sup>2,3,4</sup>, Mirjana Najdek<sup>1</sup>

1. Center for Marine Research, Ruđer Bošković Institute, Croatia

2. Department of Functional and Evolutionary Ecology, University of Vienna, Austria

3. NIOZ, Department of Marine Microbiology and Biogeochemistry, Royal Netherlands Institute for Sea Research, Utrecht University, The Netherlands

4. Vienna Metabolomics Center, University of Vienna, Austria

\*To whom correspondence should be addressed:

Marino Korlević

G. Paliaga 5, 52210 Rovinj, Croatia

Tel.: +385 52 804 768

Fax: +385 52 804 780

e-mail: marino.korlevic@irb.hr

Running title: DNA and protein isolation from macrophyte surfaces

## 1 Abstract

2 Studies of unculturable microbes often combine methods such as 16S rRNA sequencing,  
3 metagenomics and metaproteomics. To apply these techniques to the microbial community  
4 inhabiting the surfaces of marine macrophytes it is advisable to perform a selective DNA and  
5 protein isolation prior to the analysis to avoid biases due to the host material being present in high  
6 quantities. Two protocols for DNA and protein isolation were adapted for selective extractions of  
7 DNA and proteins from epiphytic communities inhabiting the surfaces of two marine macrophytes,  
8 the seagrass *Cymodocea nodosa* and the macroalga *Caulerpa cylindracea*. Protocols showed an  
9 almost complete removal of the epiphytic community regardless of the sampling season, station,  
10 settlement or host species. The obtained DNA was suitable for metagenomic and 16S rRNA  
11 sequencing, while isolated proteins could be identified by mass spectrometry. Low presence of host  
12 DNA and proteins in the samples indicated a high specificity of the protocols. The procedures are  
13 based on universally available laboratory chemicals making the protocols widely applicable. Taken  
14 together, the adapted protocols ensure an almost complete removal of the macrophyte epiphytic  
15 community. The procedures are selective for microbes inhabiting macrophyte surfaces and provide  
16 DNA and proteins applicable in 16S rRNA sequencing, metagenomics and metaproteomics.

17 **Introduction**

18 Surfaces of marine macrophytes are colonized by a diverse microbial community whose  
19 structure and function are poorly understood (Egan et al., 2013). As less than 1 % of all prokaryotic  
20 species are culturable, molecular methods such as 16S rRNA sequencing, metagenomics and  
21 metaproteomics are indispensable to study these organisms (Amann et al., 1995; Su et al., 2012).  
22 Applying these techniques requires an initial isolation step with the purpose of obtaining high  
23 quality DNA and proteins.

24 Biological material (i.e., proteins and DNA) from pelagic microbial communities is usually  
25 isolated by collecting cells onto filters and subsequently isolating the target organisms or  
26 communities (Gilbert et al., 2009). If a specific microbial size fraction is aimed sequential filtration  
27 is applied (Massana et al., 1997; Andersson et al., 2010). In contrast, obtaining microorganisms  
28 associated to surfaces require either a cell detachment procedure prior to isolation or the host  
29 material is co-extracted with the target material. Methods for separating microbial cells from the  
30 host include shaking of host tissue (Gross et al., 2003; Nõges et al., 2010), scraping of macrophyte  
31 surfaces (Uku et al., 2007) or applying ultrasonication (Weidner et al., 1996; Cai et al., 2014). It  
32 was shown that shaking alone is not sufficient to remove microbial cells from surfaces, at least  
33 not from plant root surfaces (Richter-Heitmann et al., 2016). Manual separation methods, such as  
34 scraping and brushing are time consuming and subjective, as the detachment efficiency depends  
35 on host tissue and the person performing the procedure (Cai et al., 2014). Ultrasonication was  
36 proposed as an alternative method as it is providing better results in terms of detachment efficiency  
37 (Cai et al., 2014; Richter-Heitmann et al., 2016). The downside of this procedure is that complete  
38 cell removal is still not obtained and tissue disruption was observed especially after the application  
39 of probe ultrasonication (Richter-Heitmann et al., 2016). An alternative to these cell detachment  
40 procedures is the isolation of target epiphytic compounds together with host material (Staufenberger  
41 et al., 2008; Jiang et al., 2015). This procedure can lead to problems in the following processing  
42 steps such as mitochondrial and chloroplast 16S rRNA sequence contaminations from the host

43 (Longford et al., 2007; Staufenberger et al., 2008). In addition, when performing metagenomics  
44 and metaproteomics host material can cause biased results towards more abundant host DNA and  
45 proteins.

46 An alternative to these procedures is a direct isolation of the target material by incubating  
47 macrophyte tissues in an extraction buffer. After the incubation, the undisrupted host tissue is  
48 removed followed by the isolation procedure, omitting host material contaminations. To our  
49 knowledge, the only procedure describing a direct and selective epiphytic DNA isolation from the  
50 surfaces of marine macrophytes was described by Burke et al. (2009). In contrast to previously  
51 described methods, this protocol enables an almost complete removal of the surface community.  
52 It was used for 16S rRNA gene clone library construction (Burke et al., 2011b) and metagenome  
53 sequencing (Burke et al., 2011a). This method, although providing a selective isolation procedure,  
54 uses a rapid multi-enzyme cleaner (3M) that is not available worldwide and the chemical constituents  
55 are unknown (Burke et al., 2009). Also to our knowledge, no selective isolation protocol to perform  
56 (meta)proteomics of epiphytic communities associated with marine macrophytes has been developed  
57 yet.

58 In the present study, we adapted a protocol widely used for DNA isolation from filters (Massana  
59 et al., 1997) and a protocol used for protein isolation from soils (Chourey et al., 2010; Hultman et  
60 al., 2015). These two adapted methods allowed for a selective extraction of DNA and proteins from  
61 epiphytic communities inhabiting the surfaces of two marine macrophytes, the seagrass *Cymodocea*  
62 *nodososa* and the macroalga *Caulerpa cylindracea*. In addition, we tested the removal efficiency of the  
63 protocol and the suitability of obtained DNA and proteins for 16S rRNA sequencing, metagenomics  
64 and metaproteomics.

65 **Materials and methods**

66 **Sampling**

67 Leaves of *C. nodosa* were sampled in a *C. nodosa* meadow in the Bay of Saline, northern  
68 Adriatic Sea (45°7'5" N, 13°37'20" E) and in a *C. nodosa* meadow invaded by *C. cylindracea* in  
69 the Bay of Funtana, northern Adriatic Sea (45°10'39" N, 13°35'42" E). Thalli of *C. cylindracea*  
70 were sampled in the same *C. nodosa* invaded meadow in the Bay of Funtana and at a locality of  
71 only *C. cylindracea* located in the proximity of the invaded meadow. Leaves and thalli for 16S  
72 rRNA analysis, metagenomics and metaproteomics were collected in two contrasting seasons, on 4  
73 December 2017 (16S rRNA analysis and metaproteomics), 14 December 2017 (metagenomics) and  
74 18 June 2018 (16S rRNA analysis, metagenomics and metaproteomics). During spring 2018, the *C.*  
75 *nodosa* meadow in the Bay of Saline decayed to an extent that no leaves could be retrieved (Najdek  
76 et al., 2020). In addition, as not enough DNA for both metagenomic and 16S RNA analysis were  
77 obtained during the sampling on 4 December 2017, an additional sampling on 14 December 2017  
78 was carried out in the Bay of Funtana. Leaves and thalli were collected by diving and transported to  
79 the laboratory in containers placed on ice and filled with seawater from this site. Upon arrival to the  
80 laboratory, *C. nodosa* leaves were cut into sections of 1 – 2 cm, while *C. cylindracea* thalli were  
81 cut into 5 – 8 cm long sections. Leaves and thalli were washed three times with sterile artificial  
82 seawater (ASW) to remove loosely attached microbial cells.

83 **DNA isolation**

84 The DNA was isolated according to the protocol for isolation from filters described in Massana  
85 et al. (1997). This protocol was modified and adapted for microbial DNA isolation from macrophyte  
86 surfaces as described below. Five (5) ml of lysis buffer (40 mM EDTA, 50 mM Tris-HCl, 0.75 M  
87 sucrose; pH 8.3) was added to 1 g wet weight of leaves or 2 g wet-weight of thalli. For every sample,

88 duplicate isolations were performed. Lysozyme was added (final concentration 1 mg ml<sup>-1</sup>) and the  
89 mixture was incubated at 37 °C for 30 min. Subsequently, proteinase K (final concentration 0.5  
90 mg ml<sup>-1</sup>) and SDS (final concentration 1 %) were added and the samples were incubated at 55 °C  
91 for 2 h. Following the incubation, tubes were vortexed for 10 min and the mixture containing lysed  
92 epiphytic cells was separated from host leaves or thalli by transferring the solution into a clean tube.  
93 The lysate was extracted twice with a mixture of phenol:chloroform:isoamyl alcohol (25:24:1; pH 8)  
94 and once with chloroform:isoamyl alcohol (24:1). After each addition of an organic solvent mixture,  
95 tubes were slightly vortexed and centrifuged at 4,500 × g for 10 min. Following each centrifugation  
96 the aqueous phases were retrieved. After the final extraction 1/10 of chilled 3 M sodium acetate  
97 (pH 5.2) was added. DNA was precipitated by adding 1 volume of chilled isopropanol, incubating  
98 the mixtures overnight at -20 °C and centrifuging at 16,000 × g and 4 °C for 20 min. The pellet  
99 was washed twice with 1 ml of chilled 70 % ethanol and centrifuged after each washing step at  
100 20,000 × g and 4 °C for 10 min. After the first washing step duplicate pellets from the same sample  
101 were pooled and transferred to a clean 1.5 ml tube. The dried pellet was re-suspended in 100 µl of  
102 deionized water.

### 103 Illumina 16S rRNA sequencing

104 An aliquot of isolated DNA was treated with RNase A (final concentration 200 µg ml<sup>-1</sup>)  
105 for 2 h at 37 °C. The DNA concentration was determined using the Quant-iT PicoGreen  
106 dsDNA Assay Kit (Invitrogen, USA) according to the manufacturer's instructions and  
107 diluted to 1 ng µl<sup>-1</sup>. The V4 region of the 16S rRNA gene was amplified using a two-step  
108 PCR procedure. In the first PCR the 515F (5'-GTGYCAGCMGCCGCGGTAA-3') and  
109 806R (5'-GGACTACNVGGGTWTCTAAT-3') primers from the Earth Microbiome Project  
110 (<http://press.igsb.anl.gov/earthmicrobiome/protocols-and-standards/16s/>) were used to amplify  
111 the target region (Caporaso et al., 2012; Apprill et al., 2015; Parada et al., 2016). These primers  
112 contained on their 5' end a tagged sequence. Each sample was amplified in four parallel 25 µl

113 reactions of which each contained 1 × Q5 Reaction Buffer, 0.2 mM of dNTPmix, 0.7 mg ml<sup>-1</sup> BSA  
114 (Bovine Serum Albumin), 0.2 µM of forward and reverse primers, 0.5 U of Q5 High-Fidelity DNA  
115 Polymerase (New England Biolabs, USA) and 5 ng of DNA template. Cycling conditions were:  
116 initial denaturation at 94 °C for 3 min, 20 cycles of denaturation at 94 °C for 45 s, annealing at  
117 50 °C for 60 s and elongation at 72 °C for 90 s, finalized by an elongation step at 72 °C for 10  
118 min. The four parallel reactions volumes were pooled and PCR products were purified using the  
119 GeneJET PCR Purification Kit (Thermo Fisher Scientific, USA) according to the manufacturer's  
120 instructions and following the protocol that included isopropanol addition for better small DNA  
121 fragment yield. The column was eluted in 30 µl of deionized water. Purified PCR products were  
122 sent for Illumina MiSeq sequencing (2 × 250 bp) at IMGM Laboratories, Martinsried, Germany.  
123 Before sequencing at IMGM, the second PCR amplification of the two-step PCR procedure was  
124 performed using primers targeting the tagged region incorporated in the first PCR. In addition, these  
125 primers contained adapter and sample-specific index sequences. The second PCR was carried  
126 out for 8 cycles. Beside samples, a positive and negative control were sequenced. A negative  
127 control was comprised of four parallel PCR reactions without DNA template, while for a positive  
128 control a mock community composed of evenly mixed DNA material originating from 20 bacterial  
129 strains (ATCC MSA-1002, ATCC, USA) was used. Partial 16S rRNA sequences obtained in  
130 this study have been deposited in the European Nucleotide Archive (ENA) at EMBL-EBI under  
131 accession numbers SAMEA6786270, SAMEA6648792 – SAMEA6648794, SAMEA6648809 –  
132 SAMEA6648811 and SAMEA6648824.

133 Obtained sequences were analysed on the computer cluster Isabella (University Computing  
134 Center, University of Zagreb) using mothur (version 1.43.0) (Schloss et al., 2009) according to the  
135 MiSeq Standard Operating Procedure (MiSeq SOP; [https://mothur.org/wiki/MiSeq\\_SOP](https://mothur.org/wiki/MiSeq_SOP)) (Kozich et  
136 al., 2013) and recommendations given from the Riffomonas project to enhance data reproducibility  
137 (<http://www.riffomonas.org/>). For alignment and classification of sequences the SILVA SSU Ref  
138 NR 99 database (release 138; <http://www.arb-silva.de>) was used (Quast et al., 2013; Yilmaz et  
139 al., 2014). Sequences classified as chloroplasts by SILVA were exported and reclassified using

140 mothur and the RDP (<http://rdp.cme.msu.edu/>) training set (version 16) reference files adapted for  
141 mothur (Cole et al., 2014). In comparison to SILVA, RDP allows a more detailed classification of  
142 chloroplast sequences. Based on the ATCC MSA-1002 mock community included in the analysis a  
143 sequencing error rate of 0.009 % was determined, which is in line with previously reported values  
144 for next-generation sequencing data (Kozich et al., 2013; Schloss et al., 2016). In addition, the  
145 negative control processed together with the samples yielded only 2 sequences after sequence  
146 quality curation.

## 147 Metagenomics

148 Four DNA samples were selected and sent on dry ice to IMGM Laboratories, Martinsried,  
149 Germany for metagenomic sequencing. DNA was purified using AMPure XP Beads (Beckman  
150 Coulter, USA) applying a bead:DNA ratio of 1:1 (v/v), quantified with a Qubit dsDNA HS Assay  
151 Kit (Thermo Fisher Scientific, USA) and check for integrity on a 1 % agarose gel. Metagenomic  
152 sequencing libraries were generated from 300 ng of input DNA using a NEBNext Ultra II FS  
153 DNA Library Prep Kit for Illumina (New England Biolabs, USA) according to the manufacturer's  
154 instructions. Fragments were selected (500 – 700 bp) using AMPure XP Beads, PCR enriched for 3  
155 – 5 cycles and quality controlled. Libraries generated from different DNA samples were pooled and  
156 sequenced on an Illumina NovaSeq 6000 sequencing system (2 × 250 bp).

157 Obtained sequences were analysed on the Life Science Compute Cluster (LiSC) (CUBE –  
158 Computational Systems Biology, University of Vienna). Individual sequences were assembled using  
159 MEGAHIT (version 1.1.2) (Li et al., 2015) under default settings. Putative genes were predicted  
160 from contigs longer than 200 bp using Prodigal (version 2.6.3) (Hyatt et al., 2010) in metagenome  
161 mode (-p meta). Abundances of predicted genes were expressed as Reads Per Kilobase Million  
162 (RPKM) and calculated using the BWA algorithm (version 0.7.16a) (Li and Durbin, 2009). All  
163 predicted genes were functionally annotated using the eggNOG-mapper (Huerta-Cepas et al., 2017)  
164 and eggNOG database (version 5.0) (Huerta-Cepas et al., 2019). Sequence taxonomy classification

165 was determined using the lowest common ancestor algorithm adapted from DIAMOND (version  
166 0.8.36) (Buchfink et al., 2015) and by searching against the NCBI non-redundant database (NR). To  
167 determine the phylogeny, the top 10 % hits with an e-value  $< 1 \times 10^{-5}$  were used (--top 10). Sequence  
168 renaming, coverage information computing and metagenomic statistics calculations were performed  
169 using software tools from BBTools (<https://jgi.doe.gov/data-and-tools/bbtools>). Metagenomic  
170 sequences obtained in this study have been deposited in the European Nucleotide Archive (ENA) at  
171 EMBL-EBI under accession numbers SAMEA6648795, SAMEA6648797, SAMEA6648809 and  
172 SAMEA6648811.

173 **Protein isolation**

174 Proteins were isolated according to the protocol for protein isolation from soil described in  
175 Chourey et al. (2010) and modified by Hultman et al. (2015). This protocol was further modified  
176 and adapted for microbial protein isolation from macrophyte surfaces as described below. Twenty  
177 (20) ml of protein extraction buffer (4 % SDS, 100 mm Tris-HCl [pH 8.0]) was added to 5 g wet  
178 weight of leaves or 10 g wet weight of thalli. The mixture was incubated in boiling water for 5  
179 min, vortexed for 10 min and incubated again in boiling water for 5 min. After a brief vortex, the  
180 lysate was transferred to a clean tube separating the host leaves or thalli from the mixture containing  
181 lysed epiphytic cells. Dithiothreitol (DTT; final concentration 24 mm) was added and proteins were  
182 precipitated with chilled 100 % trichloroacetic acid (TCA; final concentration 20 %) overnight at  
183  $-20^{\circ}\text{C}$ . Precipitated proteins were centrifuged at  $10,000 \times g$  and  $4^{\circ}\text{C}$  for 40 min. The obtained  
184 protein pellet was washed three times with chilled acetone. During the first washing step the pellet  
185 was transferred to a clean 1.5 ml tube. After each washing step, samples were centrifuged at  $20,000$   
186  $\times g$  and  $4^{\circ}\text{C}$  for 5 min. Dried pellets were stored at  $-80^{\circ}\text{C}$  until further analysis.

187 **Metaproteomics**

188 Isolated proteins were whole trypsin digested using the FASP (filter-aided sample preparation)  
189 Protein Digestion Kit (Expedeon, UK) according to the manufacturer's instructions with small  
190 modifications (Wiśniewski et al., 2009). Prior to loading the solution onto the column, protein  
191 pellets were solubilized in a urea sample buffer included in the kit amended with DTT (final  
192 concentration 100 mM) for 45 min at room temperature and centrifuged at 20,000 × g for 2 – 5  
193 min at room temperature to remove larger particles. The first washing step after protein solution  
194 loading was repeated twice. In addition, the centrifugation steps were prolonged if the column  
195 was clogged. Trypsin digestion was performed on column filters at 37 °C overnight for 18 h.  
196 The final filtrate containing peptides was acidified with 1 % (final concentration) trifluoroacetic  
197 acid (TFA), freezed at –80 °C, lyophilized and sent to VIME – Vienna Metabolomics Center  
198 (University of Vienna) for metaproteomic analysis. Peptides were re-suspended in 1 % (final  
199 concentration) TFA, desalting using the Pierce C18 Tips (Thermo Fisher Scientific, USA) according  
200 to the manufacturer's instructions and sequenced on a Q Exactive Hybrid Quadrupole-Orbitrap  
201 Mass Spectrometer (Thermo Fisher Scientific, USA). Obtained MS/MS spectra were searched  
202 against a protein database composed of combined sequenced metagenomes using SEQUEST-HT  
203 engines and validated with Percolator in Proteome Discoverer 2.1 (Thermo Fisher Scientific, USA).  
204 The target-decoy approach was used to reduce the probability of false peptide identification. Results  
205 whose false discovery rate at the peptide level was < 1 % were kept. For protein identification  
206 a minimum of two peptides and one unique peptide were required. For protein quantification, a  
207 chromatographic peak area-based free quantitative method was applied.

208 **Data processing and visualization**

209 Processing and visualization of 16S rRNA, metagenomic and metaproteomic data were done  
210 using R (version 3.6.0) (R Core Team, 2019), package tidyverse (version 1.3.0) (Wickham et

211 al., 2019) and multiple other packages (Neuwirth, 2014; Xie, 2014, 2015, 2019, 2020; Wilke,  
212 2018; Xie et al., 2018; Allaire et al., 2019; Zhu, 2019; Bengtsson, 2020). The detailed analysis  
213 procedure including the R Markdown file for this paper are available as a GitHub repository  
214 ([https://github.com/MicrobesRovinj/Korlevic\\_SelectiveRemoval\\_FrontMicrobiol\\_2021](https://github.com/MicrobesRovinj/Korlevic_SelectiveRemoval_FrontMicrobiol_2021)).

215 **Confocal microscopy**

216 Host leaves and thalli from DNA and protein isolation steps were washed seven times in  
217 deionized water and fixed with formaldehyde (final concentration ~3 %). In addition, non-treated  
218 leaves and thalli, washed three times in ASW to remove loosely attached microbial cells, were fixed  
219 in the same concentration of formaldehyde and used as a positive control. For long term storage,  
220 fixed leaves and thalli were immersed in a mixture of phosphate-buffered saline (PBS) and ethanol  
221 (1:1) and stored at -20 °C. Treated and untreated segments of leaves and thalli were stained in a 2  
222 × solution of SYBR Green I and examined under a Leica TCS SP8 X FLIM confocal microscope  
223 (Leica Microsystems, Germany).

224 **Results**

225 To assess the removal efficiency of the DNA and protein isolation procedures, leaves and thalli  
226 were examined under a confocal microscope before and after treatments were performed. The  
227 modified procedures resulted in an almost complete removal of the surface community of both, *C.*  
228 *nodosa* and *C. cylindracea*. In addition, a similar removal efficiency was observed for communities  
229 sampled in contrasting months, December 2017 (Fig. 1) and June 2018 (Fig. 2). Also, no effect of  
230 station, settlement or isolation procedure (DNA or protein) on the removal efficiency was observed  
231 (Figs. 1 and 2).

232 To evaluate whether the obtained DNA is suitable to determine the composition of the microbial  
233 community Illumina sequencing of the V4 region of the 16S rRNA was performed. Sequencing  
234 yielded a total of 336,944 sequences after quality curation and exclusion of eukaryotic, mitochondrial  
235 and no relative sequences. The number of sequences classified as chloroplasts was 97,334. After  
236 excluding these sequences, the total number of retrieved reads was 239,610, ranging from 22,596  
237 to 52,930 sequences per sample (Table S1). Even when the highest sequencing effort was applied,  
238 the rarefaction curves did not level off which is commonly observed in high-throughput 16S rRNA  
239 amplicon sequencing (Fig. S1). Sequences clustering at a similarity level of 97 % yielded a total of  
240 8,355 different OTUs. Taxonomic classification of reads revealed a macrophyte-associated epiphytic  
241 community that mainly composed of *Alphaproteobacteria* ( $14.9 \pm 3.5 \%$ ), *Bacteroidota* ( $12.5 \pm 2.4 \%$ ),  
242 *Gammaproteobacteria* ( $11.6 \pm 4.3 \%$ ), *Desulfobacterota* ( $7.8 \pm 7.5 \%$ ), *Cyanobacteria* ( $6.5 \pm 4.7 \%$ ) and *Planctomycetota* ( $2.9 \pm 1.7 \%$ ) (Fig. 3).

244 Primers used in this study, as in many other 16S rRNA amplicon procedures, also amplified  
245 chloroplast 16S rRNA genes. We observed a high proportion of chloroplast sequences in all analysed  
246 samples ( $33.4 \pm 9.4 \%$ ) (Fig. 3). To determine whether chloroplast sequences originate from  
247 the host or eukaryotic epiphytic organisms, we exported SILVA-classified chloroplast sequences  
248 and reclassified them using the RDP (Ribosomal Database Project) training set that allows for

249 a more detailed chloroplast classification. The largest proportion of sequences was classified as  
250 Bacillariophyta ( $89.7 \pm 5.7\%$ ) indicating that the DNA removal procedure resulted in only minor  
251 co-extracted quantities of host DNA (Fig. 4). Chloroplast sequences classified as Streptophyta  
252 constituted  $3.3 \pm 2.8\%$  of all chloroplast sequences originating from *C. nodosa* samples, while  
253 sequences classified as Chlorophyta comprised only  $0.02 \pm 0.01\%$  of all chloroplast sequences  
254 associated with *C. cylindracea* samples.

255 To determine whether the extracted DNA can be used for metagenomic sequencing, four  
256 samples containing epiphytic DNA were selected and shotgun sequenced using an Illumina platform.  
257 Metagenomic sequencing yielded between 207,149,524 and 624,029,930 sequence pairs (Table S2).  
258 Obtained sequences were successfully assembled into contigs whose L50 ranged from 654 to 1,011  
259 bp. In addition, predicted coding sequences were functionally annotated (9,066,667 – 20,256,215  
260 annotated sequences; Fig. 5a) and taxonomically classified. Functional annotation allowed for an  
261 assessment of the relative contribution of each COG (Clusters of Orthologous Groups) functional  
262 category to the total number of annotated coding sequences (Fig. 5a). Functional categories  
263 containing the highest number of sequences were C (Energy production and conversion), E (Amino  
264 acid transport and metabolism), M (Cell wall/membrane/envelope biogenesis), L (Replication,  
265 recombination and repair) and P (Inorganic ion transport and metabolism). If host DNA is  
266 co-extracted with epiphytes it should be detected in large proportions in sequenced metagenomes.  
267 However, no large proportions of coding sequences classified as Streptophyta and Chlorophyta  
268 were detected (Table S3). Sequenced metagenomic DNA originating from the surface of *C. nodosa*  
269 contained 1.3 % of coding sequences classified as Streptophyta in December 2017 and 0.7 % in June  
270 2018. Furthermore, the summed RPKM (Reads Per Kilobase Million) of these sequences constituted  
271 1.7 % of total RPKM of all successfully classified sequences in December 2017 and 1.1 % in June  
272 2018. Similar low proportions of host coding sequences were detected in metagenomic samples  
273 originating from the surfaces of *C. cylindracea*. Of all successfully classified coding sequences 0.2  
274 % were classified as Chlorophyta in December 2017 and 0.1 % in June 2018. A relatively higher  
275 proportion of RPKM of these sequences than in the case of *C. nodosa* was observed, indicating

276 a higher co-extraction of host DNA in *C. cylindracea*. In December, the proportion of RPKM of  
277 sequences classified as Chlorophyta was 8.2 %, while in June 2018 it reached 13.6 %.

278 To evaluate whether the procedure for protein extraction is suitable for metaproteomic analysis,  
279 obtained proteins were trypsin digested and sequenced using a mass spectrometer. Obtained  
280 MS/MS spectra were searched against a protein database from sequenced metagenomes. From  
281 14,219 to 16,449 proteins were identified in isolated protein samples (Fig. 5b). In addition,  
282 successful identification of proteins allowed for an assessment of the relative contribution of  
283 each COG functional category to the total number of identified proteins (Fig. 5b). Functional  
284 categories containing the highest number of identified proteins were C (Energy production and  
285 conversion), G (Carbohydrate transport and metabolism), P (Inorganic ion transport and metabolism),  
286 O (Posttranslational modification, protein turnover, chaperones) and E (Amino acid transport and  
287 metabolism). Isolated proteins could originate from epiphytic organisms inhabiting the macrophyte  
288 surface and/or from macrophyte tissue underlying them. The contribution of proteins originating  
289 from host tissues was evaluated by identifying all the proteins predicted to belong to any taxonomic  
290 group within the phyla Streptophyta and Chlorophyta and by calculating their contribution to the  
291 number and abundance (NAAF – Normalized Abundance Area Factor) of all identified proteins.  
292 On average, proteins isolated from the surface of *C. nodosa* contained  $1.8 \pm 0.06$  % of proteins  
293 associated with Streptophyta, contributing to  $2.2 \pm 0.8$  % of total proteins. Similar to metagenomes,  
294 proteins associated with Chlorophyta contributed more to *C. cylindracea* than proteins associated  
295 with Streptophyta to *C. nodosa*. Chlorophyta associated proteins comprised  $5.2 \pm 0.06$  % of all  
296 identified proteins in *C. cylindracea*, contributing  $19.2 \pm 1.5$  % to the total protein abundance.

297 **Discussion**

298 To test whether the developed DNA and protein isolation protocols efficiently detach microbes  
299 from the macrophyte surface we selected *C. nodosa* and *C. cylindracea* as representatives of seagrass  
300 and macroalgal species. These species differ morphologically. While *C. nodosa* leaves are flat, *C.*  
301 *cylindracea* thalli are characterized by an uneven surface (Kuo and den Hartog, 2001; Verlaque et  
302 al., 2003). The developed protocol led to an almost complete removal of epiphytic cells from the  
303 surfaces of both species comparable to the result of Burke et al. (2009), indicating that structural  
304 differences do not impact the removal efficiency. In addition, isolation protocols were tested in two  
305 contrasting seasons, as it is known that macrophytes are harbouring more algal epiphytes during  
306 autumn and winter (Reyes and Sansón, 2001). No differences in the removal efficiency was observed  
307 between seasons suggesting that these protocols can be used on macrophyte samples retrieved  
308 throughout the year. Also, no removal differences were observed on samples derived from the same  
309 host but from different locations.

310 Successful amplification and sequencing of the V4 region of the 16S rRNA gene proved that the  
311 isolated DNA can be used to estimate the microbial epiphytic diversity. Taxonomic groups detected  
312 in this step can also be often found in epiphytic communities associated with other macrophytes  
313 (Burke et al., 2011b; Morrissey et al., 2019). A problem often encountered in studies focusing on  
314 epiphytic communities is the presence of large proportions of chloroplast 16S rRNA sequences in  
315 the pool of amplified molecules, especially if the epiphytic DNA was isolated without prior selection  
316 (Staufenberger et al., 2008). These sequences can derive from host chloroplasts or from eukaryotic  
317 epiphytic chloroplast DNA. Although the proportion of obtained chloroplast 16S rRNA sequences  
318 in our samples was substantial, they derived almost exclusively from eukaryotic epiphytes. High  
319 proportion of chloroplast 16S rRNA sequences in studies applying selective procedures that include  
320 direct cellular lysis on host surfaces were observed before (Michelou et al., 2013). It is possible that  
321 chloroplast-specific sequences even in these studies originated from eukaryotic epiphytic cells and  
322 not from host chloroplasts. Indeed, it is common during 16S rRNA profiling of pelagic microbial

323 communities to observe high proportions of chloroplast sequences (Gilbert et al., 2009; Korlević  
324 et al., 2016). In addition, a very low proportion of chloroplast 16S rRNA sequences in samples  
325 originating from *C. cylindracea* in comparison to *C. nodosa* could be explained by the presence of  
326 three introns in the gene for 16S rRNA in some members of the genus *Caulerpa* that could hamper  
327 the amplification process (Lam and Lopez-Bautista, 2016).

328 High quality DNA is also needed for metagenomics. The obtained number of metagenomic  
329 sequences and assembly statistics were comparable to metagenomes and metatranscriptomes derived  
330 from similar surface associated communities (Crump et al., 2018; Cúcio et al., 2018). In addition,  
331 functional annotation of predicted coding sequences to COG functional categories showed that  
332 the obtained metagenomes can be used to determine the metabolic capacity of surface associated  
333 communities (Leary et al., 2014; Cúcio et al., 2018). The proportion of coding sequences, including  
334 their RPKM, originating from *C. nodosa* metagenomes and classified as Streptophyta was low  
335 indicating that the isolation procedure was specific for epiphytic cells. DNA samples isolated from  
336 the surface of *C. cylindracea* exhibited a low proportion of Chlorophyta coding sequences, however,  
337 their RPKM was higher than in the samples originating from *C. nodosa*. One of the reasons for this  
338 elevated RPKM of Chlorophyta sequences in *C. cylindracea* could be the differences in the tissue  
339 structure between these two host species. While *C. nodosa* leaves are composed of individual cells,  
340 the thallus of *C. cylindracea* is, like in other siphonous algal species, composed of a single large  
341 multinucleate cell (Coneva and Chitwood, 2015). The absence of individual cells in *C. cylindracea*  
342 could cause a leakage of genetic material into the extraction buffer causing an elevated presence of  
343 host sequences in the samples for metagenome analyses.

344 To obtain insight into the metabolic status of uncultivated prokaryotes, a metaproteomic  
345 approach is required (Saito et al., 2019). The applied protocol for epiphytic protein isolation  
346 followed by a metaproteomic analysis identified between 14,219 and 16,449 proteins, which is  
347 higher than previously reported for e.g. soils (Chourey et al., 2010; Hultman et al., 2015), seawater  
348 (Williams et al., 2012) and biofilms (Leary et al., 2014). The functional annotation of identified

349 proteins into COG functional categories showed that the protein isolation protocol can be used to  
350 assess the metabolic status of the epiphytic community (Leary et al., 2014). Similar to the results of  
351 the metagenomic analysis, the number and abundance of identified proteins affiliated to Streptophyta  
352 in *C. nodosa* samples were low, indicating that the procedure is selective for epiphytic cell proteins.  
353 In addition, a higher number and abundance of identified proteins associated with Chlorophyta were  
354 observed in *C. cylindracea* samples. The cause of this elevated presence of Chlorophyta-associated  
355 proteins can be, similar to the DNA isolation protocol, explained by the absence of individual cells  
356 in this siphonous alga (Coneva and Chitwood, 2015).

357 In conclusion, the developed protocols for DNA and protein isolation from macrophyte surfaces  
358 almost completely remove the epiphytic community from both, *C. nodosa* and *C. cylindracea*, in  
359 different seasons. Also, the obtained DNA and proteins are suitable for 16S rRNA sequencing,  
360 metagenomics and metaproteomics analyses while the obtained material contains low quantities of  
361 host DNA and proteins making the protocols specific for epiphytes. Furthermore, the protocols are  
362 based on universally available laboratory chemicals hence, making them widely applicable.

## 363 Acknowledgements

364 This work was funded by the Croatian Science Foundation through the MICRO-SEAGRASS  
365 project (project number IP-2016-06-7118). ZZ and GJH were supported by the Austrian Science  
366 Fund (FWF) project ARTEMIS (project number P28781-B21). We would like to thank Margareta  
367 Buterer for technical support, Paolo Paliaga for help during sampling, Lucija Horvat for technical  
368 support in confocal microscopy, Dušica Vujaklija for help in accessing the confocal microscope  
369 and Sonja Tischler for technical support in mass spectrometry. In addition, we would like to thank  
370 the University Computing Center of the University of Zagreb for access to the computer cluster  
371 Isabella and CUBE – Computational Systems Biology of the University of Vienna for access to the  
372 Life Science Compute Cluster (LiSC).

373 **References**

- 374 Allaire, J. J., Xie, Y., McPherson, J., Luraschi, J., Ushey, K., Atkins, A., et al. (2019).
- 375 *remarkdown: Dynamic documents for R.*
- 376 Amann, R. I., Ludwig, W., and Schleifer, K. H. (1995). Phylogenetic identification and *in situ*  
377 detection of individual microbial cells without cultivation. *Microbiol. Rev.* 59, 143–169.
- 378 Andersson, A. F., Riemann, L., and Bertilsson, S. (2010). Pyrosequencing reveals contrasting  
379 seasonal dynamics of taxa within Baltic Sea bacterioplankton communities. *ISME J.* 4, 171–181.  
380 doi:10.1038/ismej.2009.108.
- 381 Apprill, A., McNally, S., Parsons, R., and Weber, L. (2015). Minor revision to V4 region SSU  
382 rRNA 806R gene primer greatly increases detection of SAR11 bacterioplankton. *Aquat. Microb.*  
383 *Ecol.* 75, 129–137. doi:10.3354/ame01753.
- 384 Bengtsson, H. (2020). *matrixStats: Functions that apply to rows and columns of matrices (and*  
385 *to vectors).*
- 386 Buchfink, B., Xie, C., and Huson, D. H. (2015). Fast and sensitive protein alignment using  
387 DIAMOND. *Nat. Methods* 12, 59–60. doi:10.1038/nmeth.3176.
- 388 Burke, C., Kjelleberg, S., and Thomas, T. (2009). Selective extraction of bacterial DNA from  
389 the surfaces of macroalgae. *Appl. Environ. Microbiol.* 75, 252–256. doi:10.1128/AEM.01630-08.
- 390 Burke, C., Steinberg, P., Rusch, D., Kjelleberg, S., and Thomas, T. (2011a). Bacterial  
391 community assembly based on functional genes rather than species. *Proc. Natl. Acad. Sci.*  
392 *U. S. A.* 108, 14288–14293. doi:10.1073/pnas.1101591108.

393 Burke, C., Thomas, T., Lewis, M., Steinberg, P., and Kjelleberg, S. (2011b). Composition,  
394 uniqueness and variability of the epiphytic bacterial community of the green alga *Ulva australis*.  
395 *ISME J.* 5, 590–600. doi:10.1038/ismej.2010.164.

396 Cai, X., Gao, G., Yang, J., Tang, X., Dai, J., Chen, D., et al. (2014). An ultrasonic method for  
397 separation of epiphytic microbes from freshwater submerged macrophytes. *J. Basic Microbiol.* 54,  
398 758–761. doi:10.1002/jobm.201300041.

399 Caporaso, J. G., Lauber, C. L., Walters, W. A., Berg-Lyons, D., Huntley, J., Fierer, N., et al.  
400 (2012). Ultra-high-throughput microbial community analysis on the Illumina HiSeq and MiSeq  
401 platforms. *ISME J.* 6, 1621–1624. doi:10.1038/ismej.2012.8.

402 Chourey, K., Jansson, J., VerBerkmoes, N., Shah, M., Chavarria, K. L., Tom, L. M., et al.  
403 (2010). Direct cellular lysis/protein extraction protocol for soil metaproteomics. *J. Proteome Res.* 9,  
404 6615–6622. doi:10.1021/pr100787q.

405 Cole, J. R., Wang, Q., Fish, J. A., Chai, B., McGarrell, D. M., Sun, Y., et al. (2014). Ribosomal  
406 Database Project: Data and tools for high throughput rRNA analysis. *Nucleic Acids Res* 42,  
407 D633–D642. doi:10.1093/nar/gkt1244.

408 Coneva, V., and Chitwood, D. H. (2015). Plant architecture without multicellularity:  
409 Quandaries over patterning and the soma-germline divide in siphonous algae. *Front. Plant Sci.* 6,  
410 287. doi:10.3389/fpls.2015.00287.

411 Crump, B. C., Wojahn, J. M., Tomas, F., and Mueller, R. S. (2018). Metatranscriptomics  
412 and amplicon sequencing reveal mutualisms in seagrass microbiomes. *Front. Microbiol.* 9, 388.  
413 doi:10.3389/fmicb.2018.00388.

414 Cúcio, C., Overmars, L., Engelen, A. H., and Muyzer, G. (2018). Metagenomic analysis shows  
415 the presence of bacteria related to free-living forms of sulfur-oxidizing chemolithoautotrophic  
416 symbionts in the rhizosphere of the seagrass *Zostera marina*. *Front. Mar. Sci.* 5, 171.  
417 doi:10.3389/fmars.2018.00171.

418 Egan, S., Harder, T., Burke, C., Steinberg, P., Kjelleberg, S., and Thomas, T. (2013). The  
419 seaweed holobiont: Understanding seaweed-bacteria interactions. *FEMS Microbiol. Rev.* 37,  
420 462–476. doi:10.1111/1574-6976.12011.

421 Gilbert, J. A., Field, D., Swift, P., Newbold, L., Oliver, A., Smyth, T., et al. (2009). The  
422 seasonal structure of microbial communities in the Western English Channel. *Environ. Microbiol.*  
423 11, 3132–3139. doi:10.1111/j.1462-2920.2009.02017.x.

424 Gross, E. M., Feldbaum, C., and Graf, A. (2003). Epiphyte biomass and elemental composition  
425 on submersed macrophytes in shallow eutrophic lakes. *Hydrobiologia* 506-509, 559–565.  
426 doi:10.1023/B:HYDR.0000008538.68268.82.

427 Huerta-Cepas, J., Forsslund, K., Coelho, L. P., Szklarczyk, D., Jensen, L. J., von Mering, C., et al.  
428 (2017). Fast genome-wide functional annotation through orthology assignment by eggNOG-mapper.  
429 *Mol. Biol. Evol.* 34, 2115–2122. doi:10.1093/molbev/msx148.

430 Huerta-Cepas, J., Szklarczyk, D., Heller, D., Hernández-Plaza, A., Forsslund, S. K., Cook,  
431 H., et al. (2019). eggNOG 5.0: A hierarchical, functionally and phylogenetically annotated  
432 orthology resource based on 5090 organisms and 2502 viruses. *Nucleic Acids Res* 47, D309–D314.  
433 doi:10.1093/nar/gky1085.

434 Hultman, J., Waldrop, M. P., Mackelprang, R., David, M. M., McFarland, J., Blazewicz, S.  
435 J., et al. (2015). Multi-omics of permafrost, active layer and thermokarst bog soil microbiomes.  
436 *Nature* 521, 208–212. doi:10.1038/nature14238.

- 437 Hyatt, D., Chen, G.-L., LoCascio, P. F., Land, M. L., Larimer, F. W., and Hauser, L. J.  
438 (2010). Prodigal: Prokaryotic gene recognition and translation initiation site identification. *BMC*  
439 *Bioinformatics* 11, 119. doi:10.1186/1471-2105-11-119.
- 440 Jiang, Y.-F., Ling, J., Dong, J.-D., Chen, B., Zhang, Y.-Y., Zhang, Y.-Z., et al. (2015).  
441 Illumina-based analysis the microbial diversity associated with *Thalassia hemprichii* in Xincun Bay,  
442 South China Sea. *Ecotoxicology* 24, 1548–56. doi:10.1007/s10646-015-1511-z.
- 443 Korlević, M., Šupraha, L., Ljubešić, Z., Henderiks, J., Ciglenečki, I., Dautović, J., et al. (2016).  
444 Bacterial diversity across a highly stratified ecosystem: A salt-wedge Mediterranean estuary. *Syst.*  
445 *Appl. Microbiol.* 39, 398–408. doi:10.1016/j.syapm.2016.06.006.
- 446 Kozich, J. J., Westcott, S. L., Baxter, N. T., Highlander, S. K., and Schloss, P. D. (2013).  
447 Development of a dual-index sequencing strategy and curation pipeline for analyzing amplicon  
448 sequence data on the MiSeq Illumina sequencing platform. *Appl. Environ. Microbiol.* 79,  
449 5112–5120. doi:10.1128/AEM.01043-13.
- 450 Kuo, J., and den Hartog, C. (2001). “Seagrass taxonomy and identification key,” in *Global*  
451 *Seagrass Research Methods*, eds. F. T. Short and R. G. Coles (Amsterdam: Elsevier Science B.V.),  
452 31–58.
- 453 Lam, D. W., and Lopez-Bautista, J. M. (2016). Complete chloroplast genome for *Caulerpa*  
454 *racemosa* (Bryopsidales, Chlorophyta) and comparative analyses of siphonous green seaweed  
455 plastomes. *Cymbella* 2, 23–32.
- 456 Leary, D. H., Li, R. W., Hamdan, L. J., IV, W. J. H., Lebedev, N., Wang, Z., et al. (2014).  
457 Integrated metagenomic and metaproteomic analyses of marine biofilm communities. *Biofouling*  
458 30, 1211–1223. doi:10.1080/08927014.2014.977267.

- 459 Li, D., Liu, C.-M., Luo, R., Sadakane, K., and Lam, T.-W. (2015). MEGAHIT: An ultra-fast  
460 single-node solution for large and complex metagenomics assembly via succinct de Bruijn graph.  
461 *Bioinformatics* 31, 1674–1676. doi:10.1093/bioinformatics/btv033.
- 462 Li, H., and Durbin, R. (2009). Fast and accurate short read alignment with Burrows–Wheeler  
463 transform. *Bioinformatics* 25, 1754–1760. doi:10.1093/bioinformatics/btp324.
- 464 Longford, S., Tujula, N., Crocetti, G., Holmes, A., Holmström, C., Kjelleberg, S., et al. (2007).  
465 Comparisons of diversity of bacterial communities associated with three sessile marine eukaryotes.  
466 *Aquat. Microb. Ecol.* 48, 217–229. doi:10.3354/ame048217.
- 467 Massana, R., Murray, A. E., Preston, C. M., and DeLong, E. F. (1997). Vertical distribution  
468 and phylogenetic characterization of marine planktonic *Archaea* in the Santa Barbara Channel. *Appl.*  
469 *Environ. Microbiol.* 63, 50–56.
- 470 Michelou, V. K., Caporaso, J. G., Knight, R., and Palumbi, S. R. (2013). The ecology  
471 of microbial communities associated with *Macrocystis pyrifera*. *PloS One* 8, e67480.  
472 doi:10.1371/journal.pone.0067480.
- 473 Morrissey, K. L., Çavas, L., Willems, A., and De Clerck, O. (2019). Disentangling the influence  
474 of environment, host specificity and thallus differentiation on bacterial communities in siphonous  
475 green seaweeds. *Front. Microbiol.* 10, 717. doi:10.3389/fmicb.2019.00717.
- 476 Najdek, M., Korlević, M., Paliaga, P., Markovski, M., Ivančić, I., Iveša, L., et al. (2020).  
477 Dynamics of environmental conditions during the decline of a *Cymodocea nodosa* meadow.  
478 *Biogeosciences* 17, 3299–3315. doi:10.5194/bg-17-3299-2020.
- 479 Neuwirth, E. (2014). *RColorBrewer: ColorBrewer palettes*.

- 480 Nõges, T., Luup, H., and Feldmann, T. (2010). Primary production of aquatic macrophytes  
481 and their epiphytes in two shallow lakes (Peipsi and Võrtsjärv) in Estonia. *Aquat. Ecol.* 44, 83–92.  
482 doi:10.1007/s10452-009-9249-4.
- 483 Parada, A. E., Needham, D. M., and Fuhrman, J. A. (2016). Every base matters: Assessing  
484 small subunit rRNA primers for marine microbiomes with mock communities, time series and  
485 global field samples. *Environ. Microbiol.* 18, 1403–1414. doi:10.1111/1462-2920.13023.
- 486 Quast, C.,普鲁塞, E., Yilmaz, P., Gerken, J., Schweer, T., Yarza, P., et al. (2013). The SILVA  
487 ribosomal RNA gene database project: Improved data processing and web-based tools. *Nucleic  
488 Acids Res.* 41, D590–D596. doi:10.1093/nar/gks1219.
- 489 R Core Team (2019). *R: A language and environment for statistical computing*. Vienna,  
490 Austria: R Foundation for Statistical Computing.
- 491 Reyes, J., and Sansón, M. (2001). Biomass and production of the epiphytes on the leaves of  
492 *Cymodocea nodosa* in the Canary Islands. *Bot. Mar.* 44, 307–313. doi:10.1515/BOT.2001.039.
- 493 Richter-Heitmann, T., Eickhorst, T., Knauth, S., Friedrich, M. W., and Schmidt, H. (2016).  
494 Evaluation of strategies to separate root-associated microbial communities: A crucial choice in  
495 rhizobiome research. *Front. Microbiol.* 7, 773. doi:10.3389/fmicb.2016.00773.
- 496 Saito, M. A., Bertrand, E. M., Duffy, M. E., Gaylord, D. A., Held, N. A., Hervey, W. J., et  
497 al. (2019). Progress and challenges in ocean metaproteomics and proposed best practices for data  
498 sharing. *J. Proteome Res.* 18, 1461–1476. doi:10.1021/acs.jproteome.8b00761.
- 499 Schloss, P. D., Jenior, M. L., Koumpouras, C. C., Westcott, S. L., and Highlander, S. K. (2016).  
500 Sequencing 16S rRNA gene fragments using the PacBio SMRT DNA sequencing system. *PeerJ* 4,  
501 e1869. doi:10.7717/peerj.1869.

- 502 Schloss, P. D., Westcott, S. L., Ryabin, T., Hall, J. R., Hartmann, M., Hollister, E. B., et al.  
503 (2009). Introducing mothur: Open-source, platform-independent, community-supported software  
504 for describing and comparing microbial communities. *Appl. Environ. Microbiol.* 75, 7537–7541.  
505 doi:10.1128/AEM.01541-09.
- 506 Staufenberger, T., Thiel, V., Wiese, J., and Imhoff, J. F. (2008). Phylogenetic analysis  
507 of bacteria associated with *Laminaria saccharina*. *FEMS Microbiol. Ecol.* 64, 65–77.  
508 doi:10.1111/j.1574-6941.2008.00445.x.
- 509 Su, C., Lei, L., Duan, Y., Zhang, K.-Q., and Yang, J. (2012). Culture-independent methods for  
510 studying environmental microorganisms: Methods, application, and perspective. *Appl. Microbiol.*  
511 *Biotechnol.* 93, 993–1003. doi:10.1007/s00253-011-3800-7.
- 512 Uku, J., Björk, M., Bergman, B., and Díez, B. (2007). Characterization and comparison  
513 of prokaryotic epiphytes associated with three East African seagrasses. *J. Phycol.* 43, 768–779.  
514 doi:10.1111/j.1529-8817.2007.00371.x.
- 515 Verlaque, M., Durand, C., Huisman, J. M., Boudouresque, C.-F., and Le Parco, Y. (2003). On  
516 the identity and origin of the Mediterranean invasive *Caulerpa racemosa* (Caulerpales, Chlorophyta).  
517 *Eur. J. Phycol.* 38, 325–339. doi:10.1080/09670260310001612592.
- 518 Weidner, S., Arnold, W., and Puhler, A. (1996). Diversity of uncultured microorganisms  
519 associated with the seagrass *Halophila stipulacea* estimated by restriction fragment length  
520 polymorphism analysis of PCR-amplified 16S rRNA genes. *Appl. Environ. Microbiol.* 62, 766–771.
- 521 Wickham, H., Averick, M., Bryan, J., Chang, W., McGowan, L. D., François, R., et al. (2019).  
522 Welcome to the tidyverse. *J. Open Source Softw.* 4, 1686. doi:10.21105/joss.01686.
- 523 Wilke, C. O. (2018). *cowplot: Streamlined plot theme and plot annotations for 'ggplot2'*.

- 524 Williams, T. J., Long, E., Evans, F., DeMaere, M. Z., Lauro, F. M., Raftery, M. J., et al. (2012).
- 525 A metaproteomic assessment of winter and summer bacterioplankton from Antarctic Peninsula
- 526 coastal surface waters. *ISME J.* 6, 1883–1900. doi:10.1038/ismej.2012.28.
- 527 Wiśniewski, J. R., Zougman, A., Nagaraj, N., and Mann, M. (2009). Universal sample
- 528 preparation method for proteome analysis. *Nat. Methods* 6, 359–362. doi:10.1038/nmeth.1322.
- 529 Xie, Y. (2014). “knitr: A comprehensive tool for reproducible research in R,” in *Implementing*
- 530 *Reproducible Computational Research*, eds. V. Stodden, F. Leisch, and R. D. Peng (New York:
- 531 Chapman and Hall/CRC), 3–32.
- 532 Xie, Y. (2015). *Dynamic Documents with R and knitr*. 2nd ed. Boca Raton, Florida: Chapman
- 533 and Hall/CRC.
- 534 Xie, Y. (2019). TinyTeX: A lightweight, cross-platform, and easy-to-maintain LaTeX
- 535 distribution based on TeX Live. *TUGboat* 40, 30–32.
- 536 Xie, Y. (2020). *tinytex: Helper functions to install and maintain 'TeX Live', and compile*
- 537 *'LaTeX' documents*.
- 538 Xie, Y., Allaire, J. J., and Grolemund, G. (2018). *R Markdown: The Definitive Guide*. 1st ed.
- 539 Boca Raton, Florida: Chapman and Hall/CRC.
- 540 Yilmaz, P., Parfrey, L. W., Yarza, P., Gerken, J., Pruesse, E., Quast, C., et al. (2014). The
- 541 SILVA and "All-Species Living Tree Project (LTP)" taxonomic frameworks. *Nucleic Acids Res.* 42,
- 542 D643–D648. doi:10.1093/nar/gkt1209.
- 543 Zhu, H. (2019). *kableExtra: Construct complex table with 'kable' and pipe syntax*.

544 **Figure legends**

545 **Fig. 1.** Confocal microscope images of *C. nodosa* and *C. cylindracea* surfaces from the Bay of  
546 Saline and the Bay of Funtana (mixed and monospecific settlements) sampled on 4 December 2017  
547 and stained with SYBR Green I. Scale bar at all images is 60  $\mu$ m.

548 **Fig. 2.** Confocal microscope images of *C. nodosa* and *C. cylindracea* surfaces from the Bay of  
549 Funtana (mixed and monospecific settlements) sampled on 19 June 2018 and stained with SYBR  
550 Green I. Scale bar at all images is 60  $\mu$ m.

551 **Fig. 3.** Taxonomic classification and relative contribution of the most abundant ( $\geq 1\%$ ) bacterial  
552 and archaeal sequences from surfaces of two marine macrophytes (*C. nodosa* and *C. cylindracea*)  
553 sampled in the Bay of Saline and the Bay of Funtana (mixed and monospecific settlements) and in  
554 two contrasting seasons (4 December 2017 and 19 June 2018).

555 **Fig. 4.** Taxonomic classification and relative contribution of chloroplast sequences from surfaces of  
556 two marine macrophytes (*C. nodosa* and *C. cylindracea*) sampled in the Bay of Saline and the Bay  
557 of Funtana (mixed and monospecific settlements) and in two contrasting seasons (4 December 2017  
558 and 19 June 2018).

559 **Fig. 5.** Relative contribution of each COG category to the total number of annotated coding  
560 sequences (A) from metagenomes and identified proteins (B) from metaproteomes associated with  
561 surfaces of two marine macrophytes (*C. nodosa* and *C. cylindracea*) sampled in the Bay of Saline  
562 and the Bay of Funtana (mixed and monospecific settlements) and in two contrasting seasons (4/14  
563 December 2017 and 19 June 2018). Total number of annotated coding sequences and identified  
564 proteins is given above the corresponding bar.

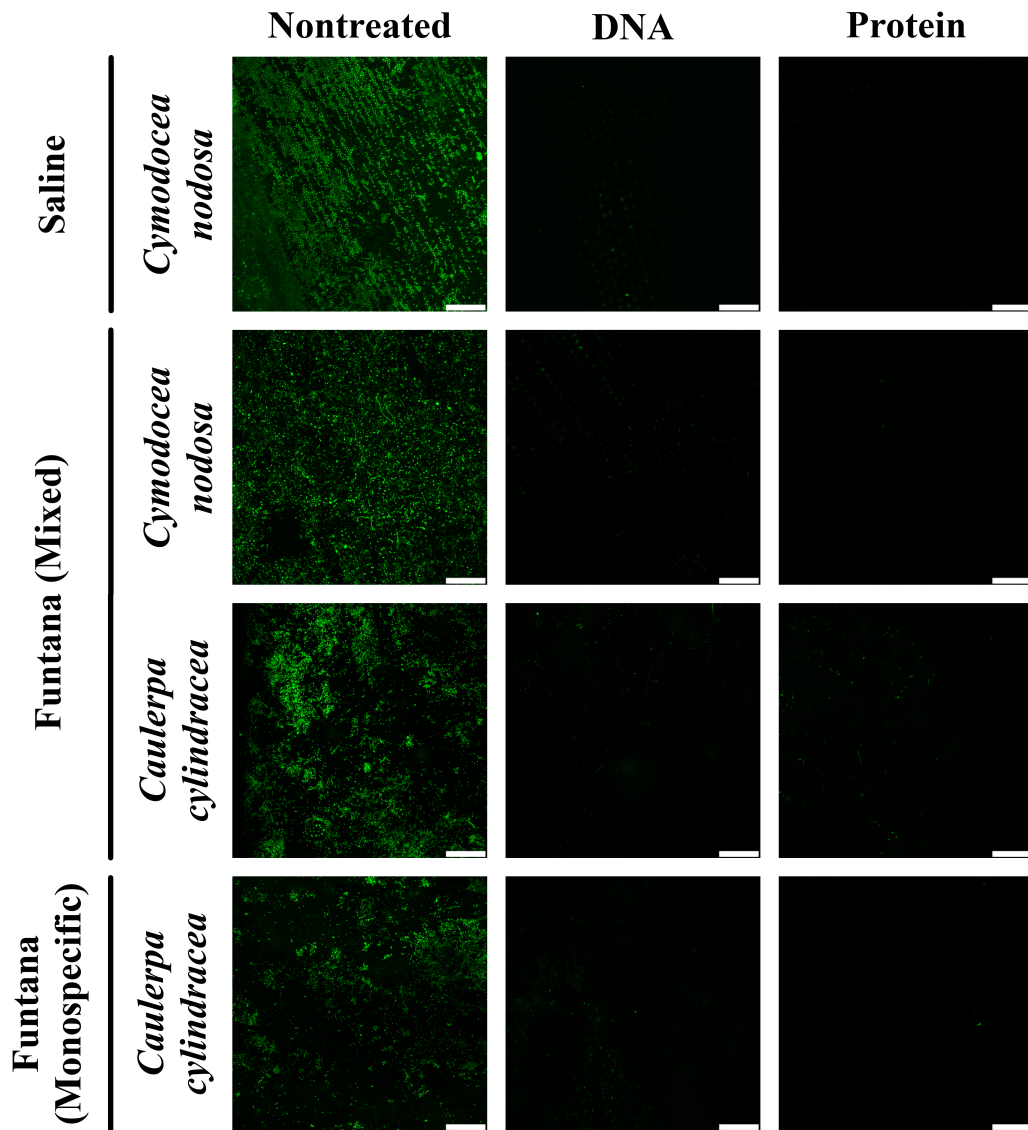


**Fig. 1.** Confocal microscope images of *C. nodosa* and *C. cylindracea* surfaces from the Bay of Saline and the Bay of Funtana (mixed and monospecific settlements) sampled on 4 December 2017 and stained with SYBR Green I. Scale bar at all images is 60  $\mu$ m.

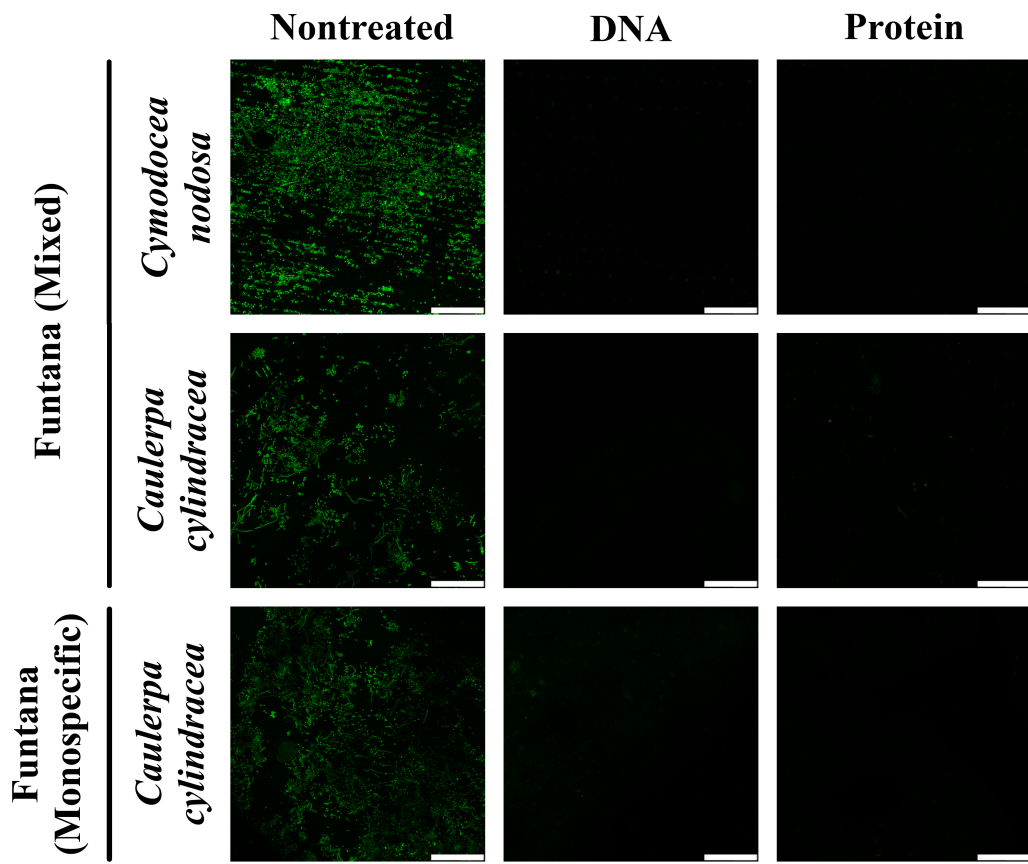


**Fig. 2.** Confocal microscope images of *C. nodosa* and *C. cylindracea* surfaces from the Bay of Funtana (mixed and monospecific settlements) sampled on 19 June 2018 and stained with SYBR Green I. Scale bar at all images is 60  $\mu$ m.

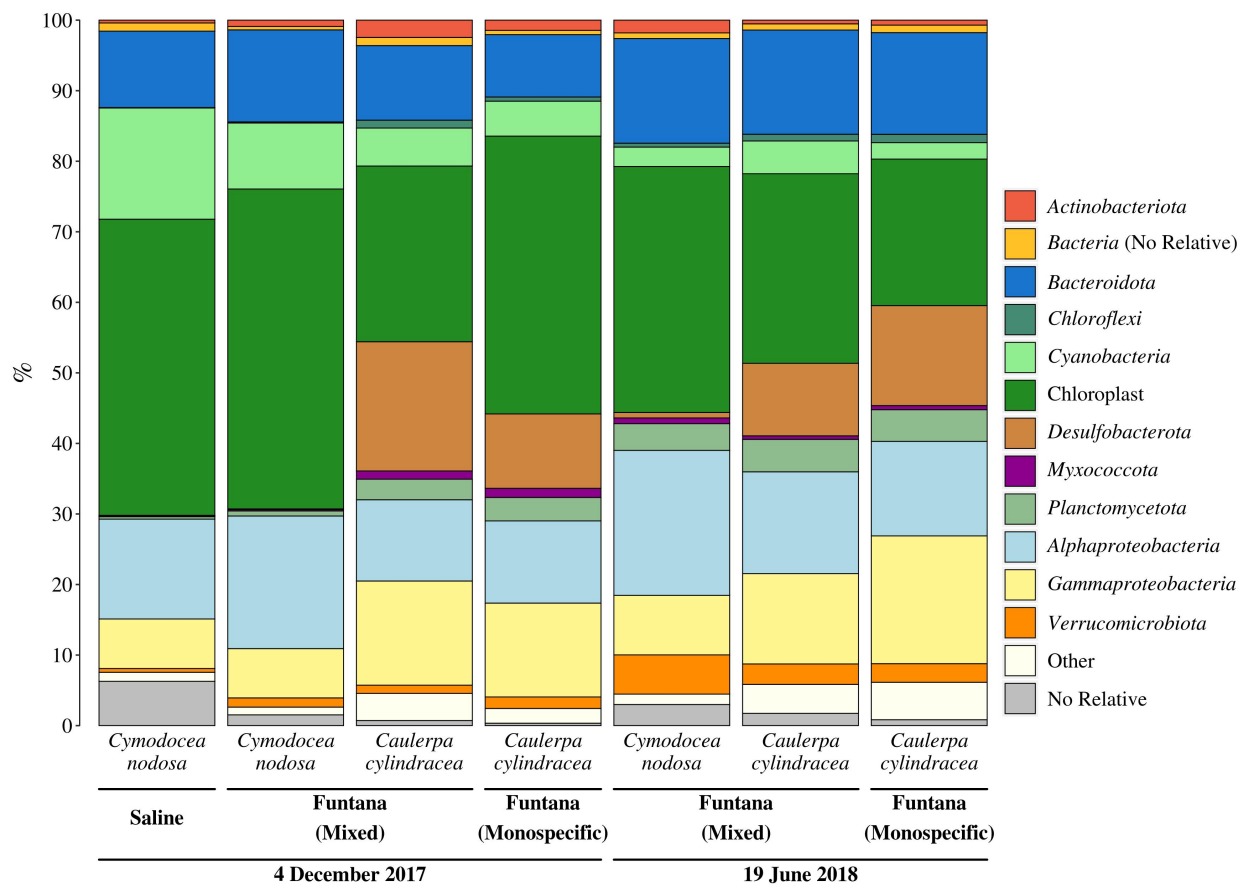


**Fig. 3.** Taxonomic classification and relative contribution of the most abundant ( $\geq 1\%$ ) bacterial and archaeal sequences from surfaces of two marine macrophytes (*C. nodosa* and *C. cylindracea*) sampled in the Bay of Saline and the Bay of Funtana (mixed and monospecific settlements) and in two contrasting seasons (4 December 2017 and 19 June 2018).

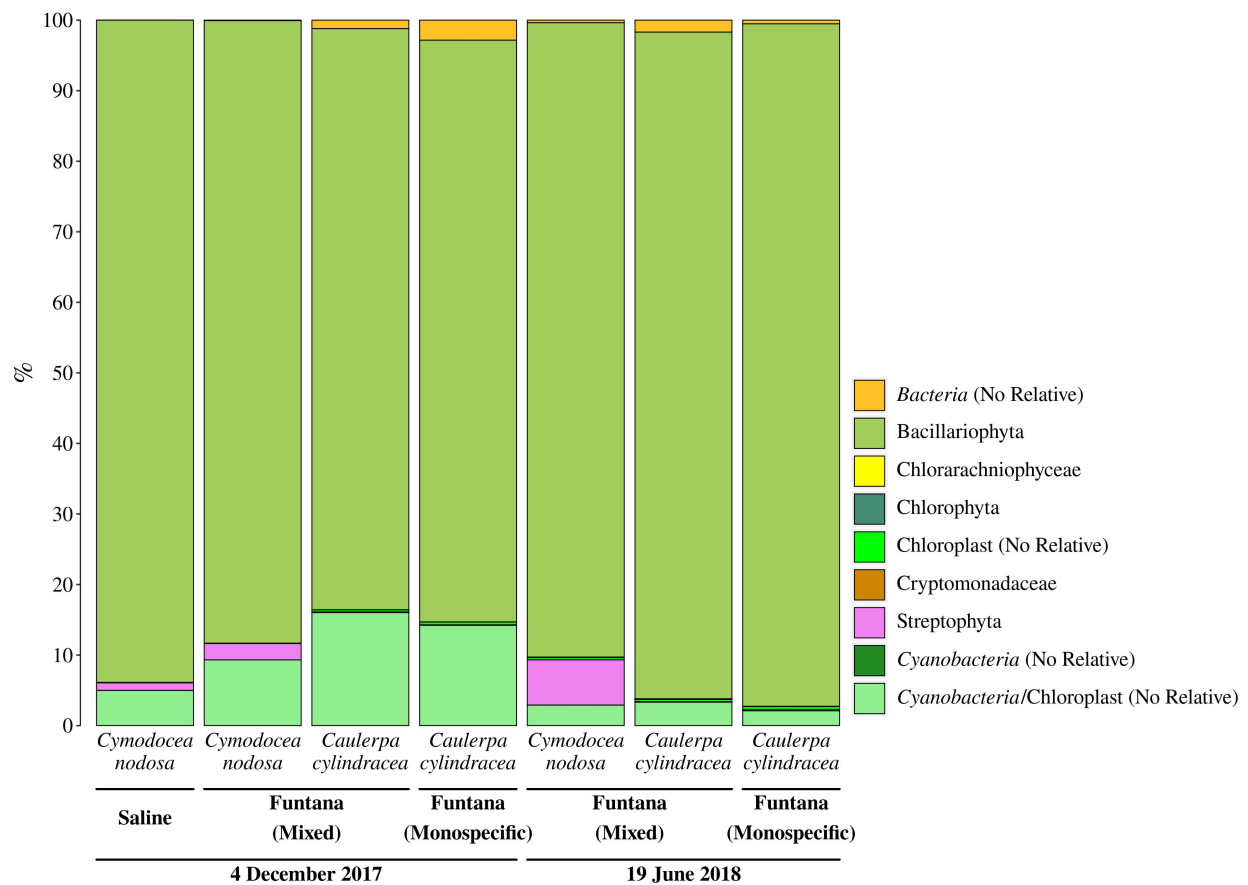


**Fig. 4.** Taxonomic classification and relative contribution of chloroplast sequences from surfaces of two marine macrophytes (*C. nodosa* and *C. cylindracea*) sampled in the Bay of Saline and the Bay of Funtana (mixed and monospecific settlements) and in two contrasting seasons (4 December 2017 and 19 June 2018).

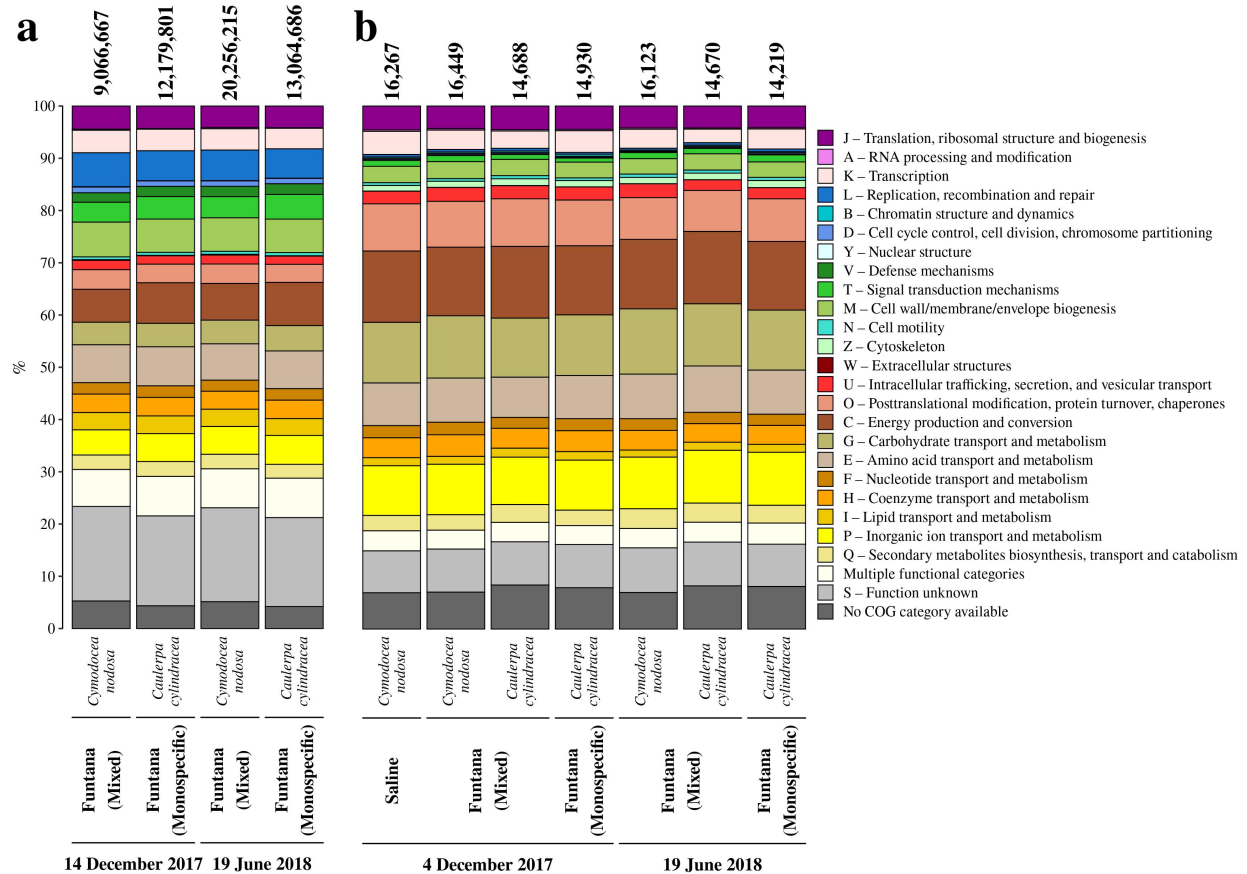


**Fig. 5.** Relative contribution of each COG category to the total number of annotated coding sequences (A) from metagenomes and identified proteins (B) from metaproteomes associated with surfaces of two marine macrophytes (*C. nodosa* and *C. cylindracea*) sampled in the Bay of Saline and the Bay of Funtana (mixed and monospecific settlements) and in two contrasting seasons (4/14 December 2017 and 19 June 2018). Total number of annotated coding sequences and identified proteins is given above the corresponding bar.